Mesoscale Analysis of Surface Variables During the Severe Storm Outbreak of 10–11 April 1979

JEFFREY H. HOMAN[1] AND DAYTON G. VINCENT

Department of Geosciences, Purdue University, West Lafayette, IN 47907

13 July 1982 and 25 February 1983

ABSTRACT

A mesoscale analysis of surface variables is presented for an AVE–SESAME case, 10–11 April 1979, when 89 severe weather events were reported, including the Red River Valley tornado outbreak. Two severe weather outbreaks, the first along the Red River Valley and the other in north-central Texas, were found to be associated with two sub-synoptic low pressure centers. The first low formed between 1900 and 2000 GMT over the Texas Panhandle, moved eastward, and was located near Wichita Falls at 0000 GMT 11 April, the time of the deadly tornado there. It then moved slowly northeastward, having a lifetime of 7–8 hours. Barograph traces showed that a second low formed quickly at about 0120 GMT near Abilene causing additional severe storms to occur throughout the night in central Texas.

After the formation of each sub-synoptic low, moisture convergence increased in the area, creating a local environment conducive to severe storm formation. In addition, the second surge of severe weather in north-central Texas was accompanied by an eastward protrusion of the dry line. Tegtmeier's idealized sub-synoptic low (SSL) dryline wave (DLW) model agreed well with the present study. Severe thunderstorm formation occurred northeast of the SSL and also along the DLW in accordance with his conceptual model.

1. Introduction

In 1979 a field program, AVE–SESAME 1979, was established to investigate interactions between severe storms and various scales of motion. Data were collected for six individual 24-h periods between 10 April and 11 June 1979 in Texas, Oklahoma and surrounding states. The present paper concentrates on the first period, 10–11 April 1979, when 89 severe weather events, including the Red River Valley tornado outbreak and the deadly Wichita Falls tornado occurred (Alberty *et al.*, 1980). More specifically, it focuses on a detailed mesoscale analysis of surface variables just before and during outbreaks of severe weather. Since typical length and time scales of significant features that occur in our analyses are 100–200 km and a few hours, they are associated with phenomena that Orlanski (1975) has classified as meso-β scale. Before proceeding with a discussion of surface analyses, it is appropriate to note that an excellent discussion of the upper air features and mesosynoptic scale interactions for this case study has been presented by Moore and Fuelberg (1981). Other pertinent discussions of mesoscale events for this study appear in Uccellini and Kocin (1981) and Vincent and Homan (1983).

Much of the early pioneering work in mesoscale analysis was performed by Fujita and his colleagues (e.g., Fujita, 1955; Fujita *et al.*, 1956; and Tepper, 1959). In a classic paper, Fujita (1955) found that hourly surface data, supplemented by radar echoes, hourly precipitation data, and barogram and thermogram traces, provided an excellent combination for diagnosing mesoscale features. Fujita *et al.* (1956) found that intense gradients occurred in several surface variables associated with mesosystems, and that much of the severe weather was related spatially to these gradients and systems. We found that many of Fujita's techniques and ideas were invaluable in our analysis, both for the present paper and its predecessor (Vincent and Homan, 1983).

The primary objective of the present study is to provide an analysis of the temporal and spatial distributions of thermodynamic and kinematic variables at the surface just prior to and during severe storm activity. The analysis techniques are not new, but their application to an important field program case study is sufficient reason for providing timely documentation. An in-depth study of the dynamical relationships between surface features and upper air circulations was recently begun and will be presented in the future. The analysis focuses on two periods: a severe storm period associated with the formation of a sub-synoptic low pressure center, and a later severe storm period associated with the formation of a second sub-synoptic low.

[1] Current affiliation is General Software Corporation, 8401 Corporate Drive, Landover, Maryland 20785.

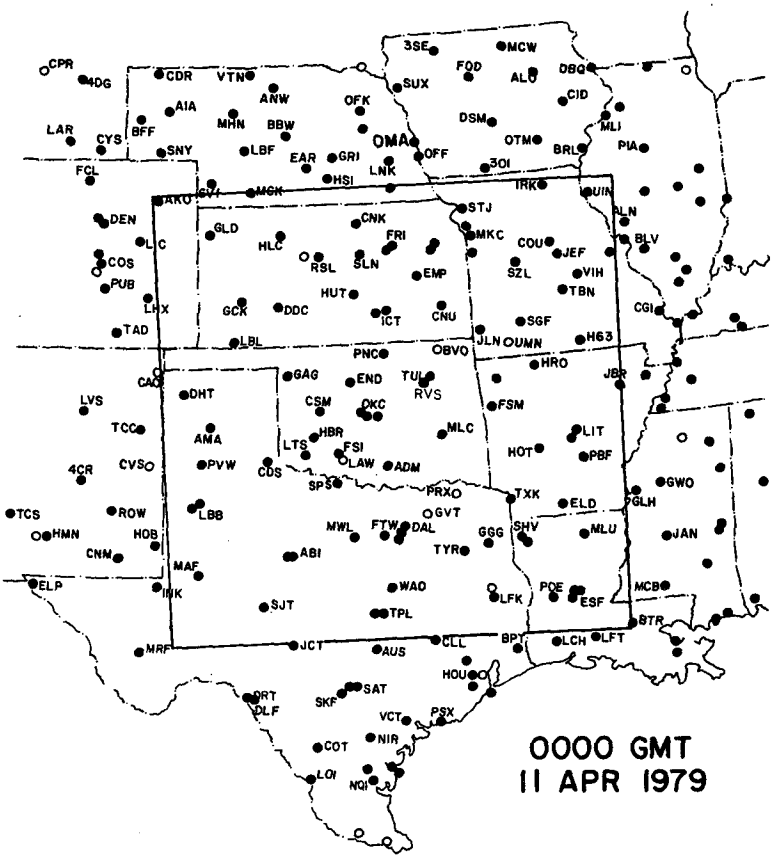

FIG. 1. Surface station density utilized for 0000 GMT 11 April 1979. Blacked-in stations represent those stations for which data were available. The square represents the boundary for the objective analysis scheme, PROAM.

2. Data reduction

Hourly surface data were analyzed subjectively from observations taken from the NWS-604 teletype circuit. These data, which were provided by Dr. Grant Darkow of the University of Missouri, include temperature, dewpoint temperature, pressure, wind, present weather and cloud information. To properly complete the mesoscale analyses of surface charts, supplemental data listed in the SESAME data users' guide, edited by Barnes (1981), were obtained. Satellite imagery was acquired from the Satellite Data Services Division EDIS/NCC/NOAA located in Washington, D.C. GOES (Geostationary Operational Experimental Satellite) East visual imagery with one kilometer resolution and at least 30 min frequency was obtained for the time period 2030 GMT 10 April through 0545 GMT 11 April 1979. Ten centimeter (10 cm) WSR-57 NWS-operated radar images were acquired from the National Climatic Center in Asheville, North Carolina. Radar sites included Monett (UMN), Missouri, Oklahoma City (OKC), Oklahoma and Stephenville (SEP), Texas. Finally, barograph traces for selected stations in Texas, Oklahoma, Kansas and Missouri were acquired from the National Climatic Center in Asheville.

Subjective analyses of the surface data mentioned above were performed to detect significant mesoscale phenomena. In addition, equivalent potential temperature, relative vorticity, velocity convergence and dewpoint temperature convergence were derived through the use of PROAM[2] (Purdue Regional Objective Analysis on the Mesoscale), since these quantities generally are good predictors of severe weather outbreaks. Fields were calculated on a 21 × 21 grid with 55 km resolution and displayed on a polar stereographic projection true at 60°N. The center of the grid is located at 35.5°N and 93°W which is slightly east of Oklahoma City. To apply PROAM a variable scanning radius is implemented which requires the influence of at least two stations to affect a grid point value. The mean station spacing is approximately 95 km. Barnes (1964) showed that an irregularly-spaced

[2] PROAM was initially implemented by Dr. Fred Leslie, now affiliated with NASA in Huntsville, AL, and a description and evaluation of the scheme appears in a NASA Technical Memorandum (Smith and Leslie, 1982).

TABLE 1. Surface station density.

Time (GMT)	Total stations	Number variables reporting			
		T	T_d	Direction/ speed	Pressure
1800	245	230	218	245	231
2000	227	216	205	226	220
2200	250	230	219	249	241
0000	250	229	219	250	240
0200	213	198	191	213	211

station array could generate "false" disturbances with wavelengths up to twice that of the mean station spacing. Therefore, an exponential weighting function was utilized (Barnes, 1964, 1973) with an arbitrary filter α chosen to effectively damp wavelengths less than 200 km. An anisotropic factor, first introduced by Endlich and Mancuso (1968), is employed to simulate the advective nature of the atmosphere by weighting observations upwind or downwind of a grid point more heavily than other stations involved in the interpolation of a value at the grid point.

Fig. 1 shows an example of the surface station density at 0000 GMT 11 April that was used in the subjective and objective analyses. Subjective analyses of the standard surface parameters were completed hourly. PROAM was utilized for each of the five times shown in Table 1, which also provides information regarding the number of reporting stations and quantity of observations.

3. Results and discussion

During the afternoon and evening of 10–11 April 1979 two swaths of storms were present. The largest swath originated southwest of Wichita Falls, Texas, in the early afternoon and tracked northeastward through the evening into Tulsa, Oklahoma. A secondary, weaker swath began in west-central Texas during the evening and tracked northeastward through the night into north-central Texas. The first outbreak along the Red River Valley contained the deadly Wichita Falls tornado. For a further analysis of tornado and F-scale intensities, see Alberty *et al.* (1980). A discussion of each of the two storm periods follows.

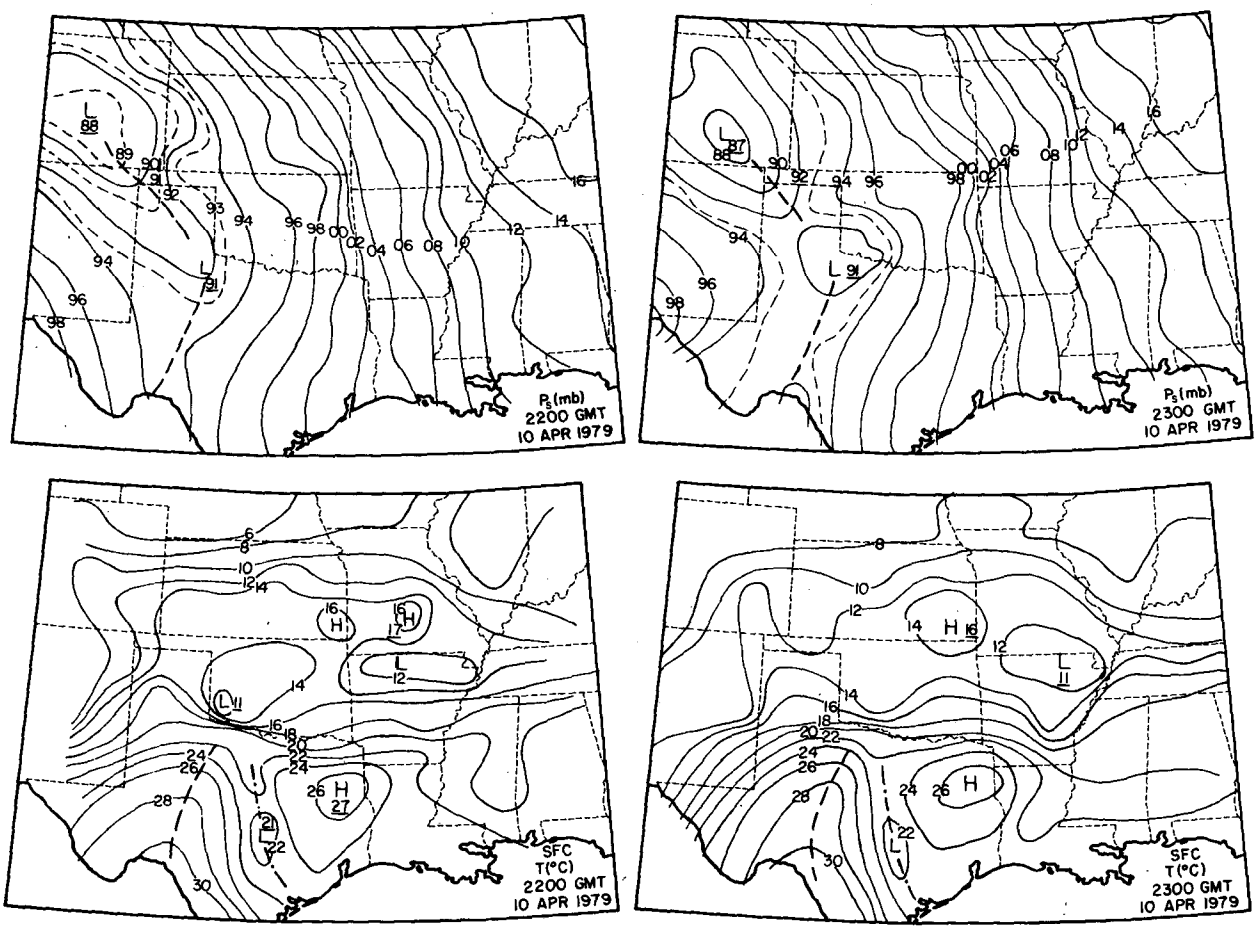

FIG. 2. Surface pressure and temperature analyses for 2200 and 2300 GMT 10 April. In temperature analyses, dashed line represents thermal ridge; dot-dash depicts axis of cool air. H, L represent maxima and minima values of variable considered.

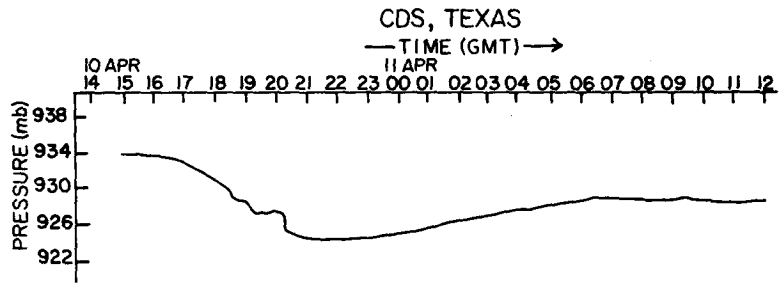

FIG. 3. Time section of pressure extracted from barograph trace for Childress (CDS), Texas.

a. Severe storm period 1: 2100–2300 GMT 10 April

Tornadic thunderstorms were first observed in north-central Texas at 2100 GMT. Fig. 2 shows the pressure and temperature fields for 2200 and 2300 GMT 10 April. One of the significant features is the appearance of a sub-synoptic low southeast of Childress, Texas. A close scrutiny of hourly charts revealed that this low formed between 1900 and 2000 GMT. To support its existence, a time section of pressure for Childress is shown in Fig. 3. A steady decrease in pressure is evident from 1600–2100 GMT as the low deepens and advances toward Childress. Additional support for the development and eventual movement of the low is given in Fig. 4, which shows the 3-h pressure tendency for 1700–2000 GMT, as well as the position of the low, dryline and winds at 2000 GMT. We shall refer to this figure in a later discussion.

Fig. 2 illustrates two significant features in the temperature field: an intense thermal ridge over west-central Texas and a tight south–north temperature gradient along the Red River Valley. For example, at 2200 GMT Wichita Falls reports a temperature of 21°C, while 30 miles to the north across the river, temperatures are nearly 10°C lower.

Dewpoint depression and wind analyses are shown in Fig. 5 for 2200 GMT. The moisture ridge extends

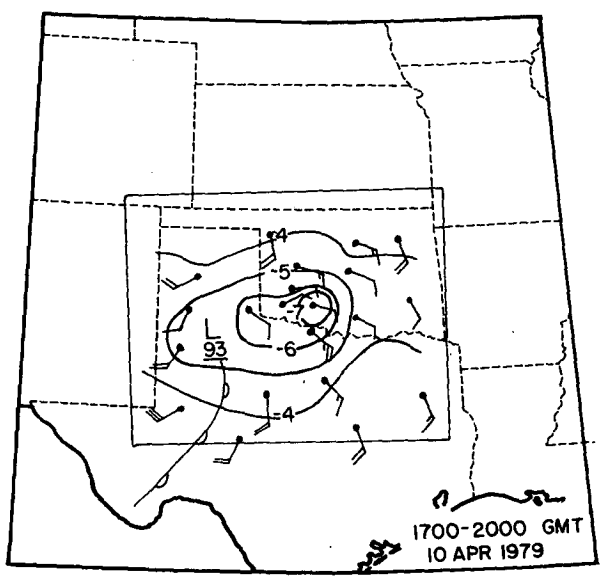

FIG. 4. Surface pressure tendency chart in mb 3 h^{-1} for 1700–2000 GMT 10 April. Winds, low pressure center and dryline are for 2000 GMT. One barb represents 5 m s^{-1}.

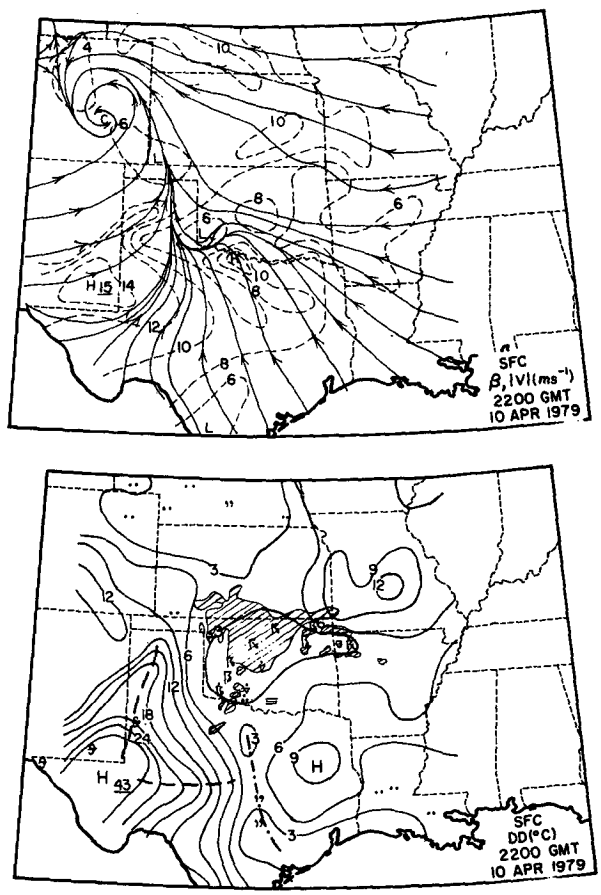

FIG. 5. Surface dewpoint depression (DD) and streamline/isotach analyses for 2200 GMT 10 April. For DD, dashed line depicts dry tongue(s); dot-dashed depicts moisture axis. Hatched areas represent radar echoes from Stephenville (SEP), Wichita (ICT) and Monett (UMN) radar sites. Solid lines on wind analyses depict streamlines; dashed lines represent isotachs. *H, L* depict maxima and minima values of variable considered.

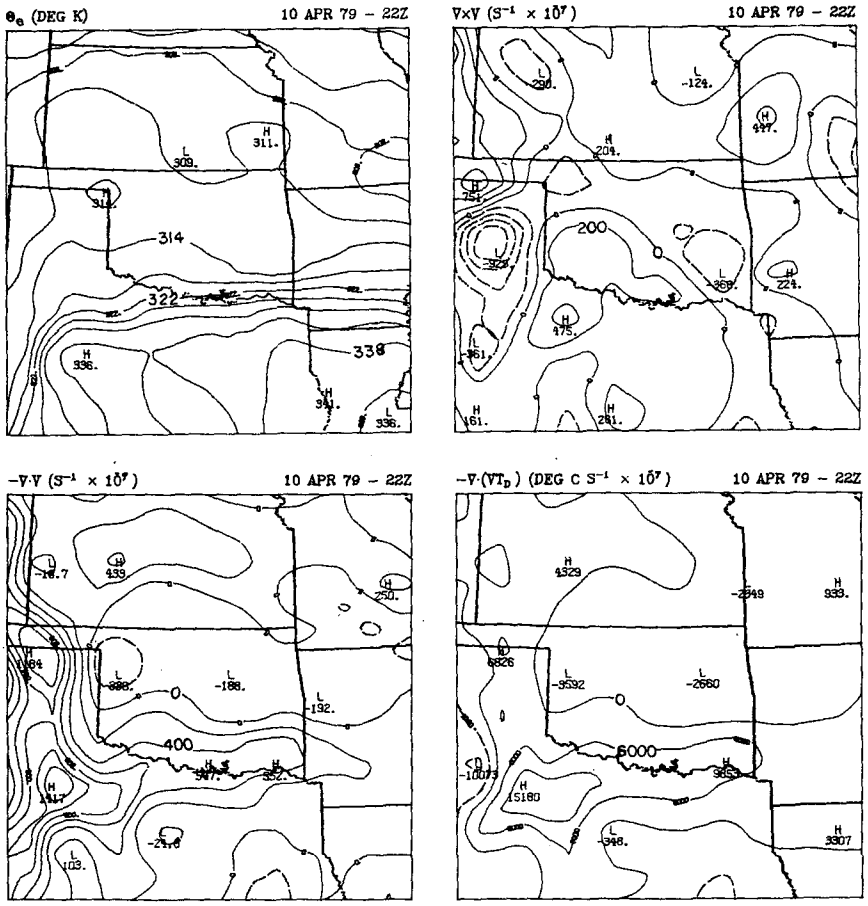

FIG. 6. Surface equivalent potential temperature θ_E (K) relative vorticity ($\nabla \times \mathbf{V}$) in 10^{-7} s^{-1}, velocity convergence ($-\nabla \cdot \mathbf{V}$) in 10^{-7} s^{-1}, and dewpoint temperature convergence ($-\nabla \cdot \mathbf{V}T_d$) in 10^{-7} °C s^{-1}, for 2200 GMT 10 April, objectively analyzed by PROAM.

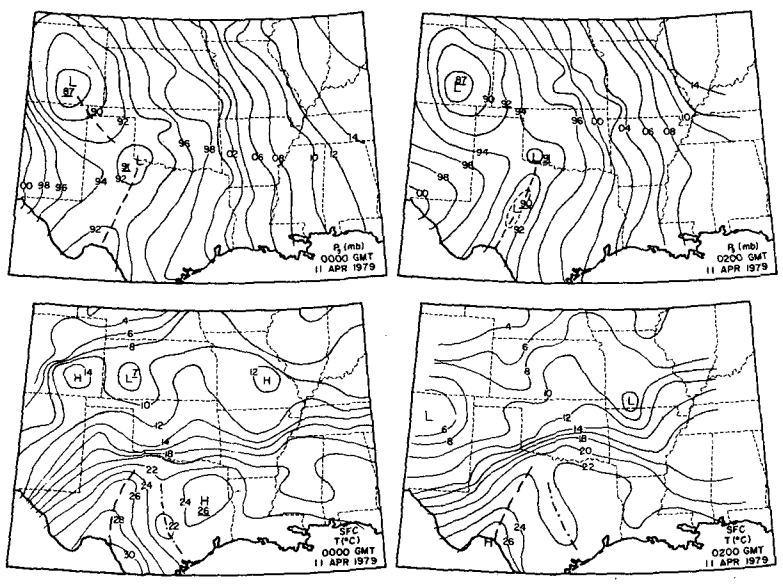

FIG. 7. Surface pressure and temperature analyses for 0000 and 0200 GMT 11 April. Variables defined as in Fig. 2.

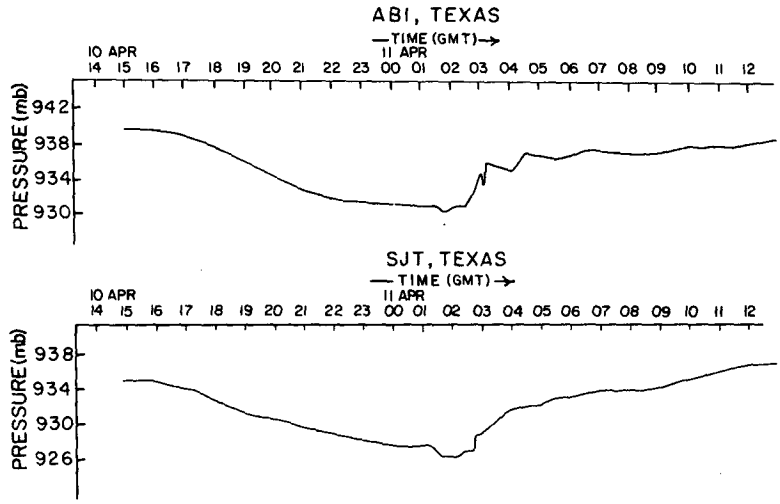

FIG. 8. Time section of pressure extracted from barograph traces for Abilene and San Angelo, Texas.

from Victoria northward to the Red River. Present weather reports and radar echoes show numerous thunderstorms and some tornadic activity. It is apparent that dry air is being advected from western Texas toward the north and east. Strong confluence in the wind field is occurring in west-central Texas in conjunction with the approaching dry line. Also note the increased thunderstorm outflow in extreme

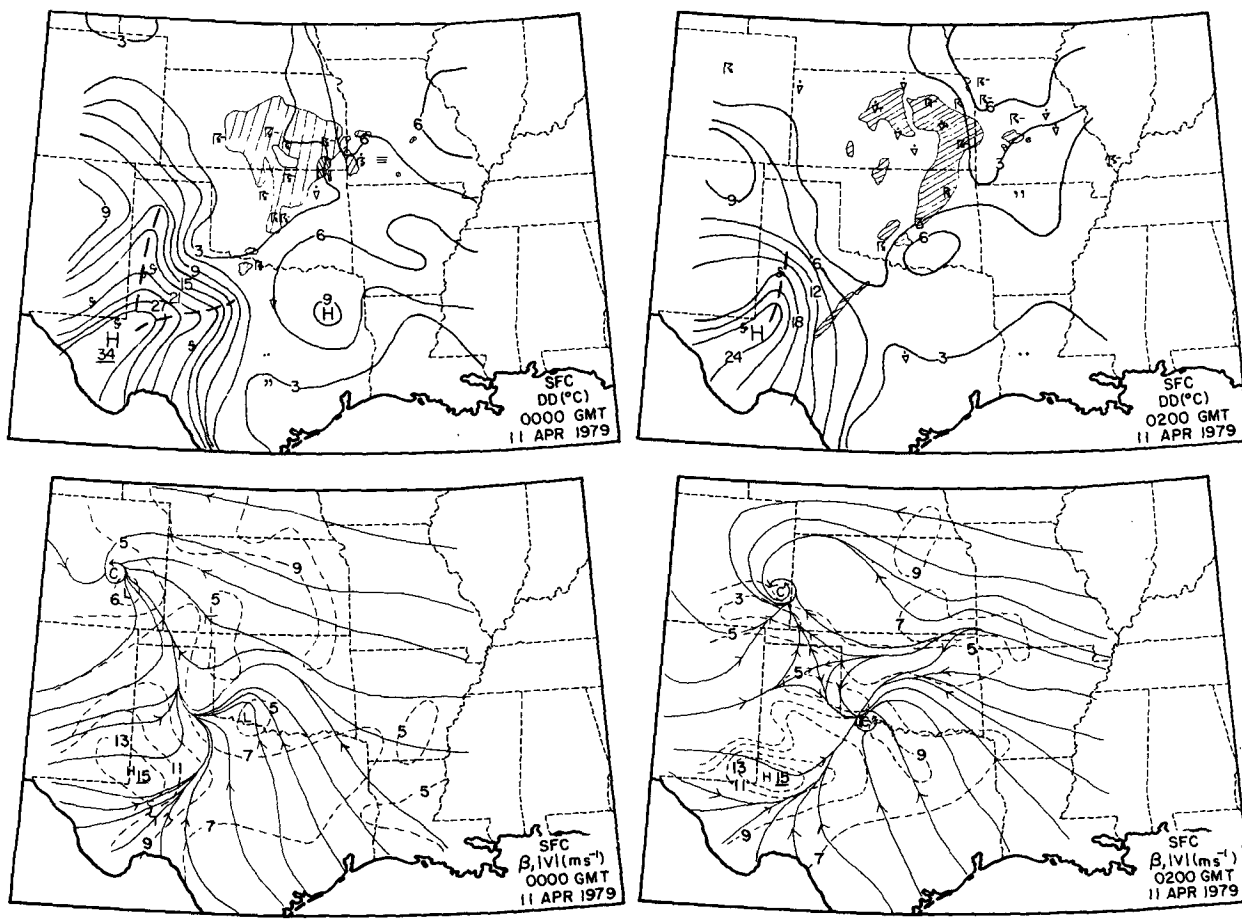

FIG. 9. Surface dewpoint depression (DD) and streamline/isotach analyses for 0000 and 0200 GMT 11 April. Variables defined as in Fig. 5.

southwest Oklahoma. A very strong low level southeasterly flow (10 m s^{-1}) is evident from Dallas northwest to Wichita Falls. In contrast, a weak northerly flow (5 m s^{-1}) is prevalent in the outflow region. Strong southwesterly flow occurs in western Texas behind the dry line.

PROAM analyses for 2200 GMT are shown in Fig. 6. The θ_E field depicts a very tight gradient along the Red River Valley and in western Texas, a reflection of the temperature field seen in Fig. 2. A comparison of the pattern in Fig. 6 to those for previous times (not shown) revealed that the region of strongest gradient has moved northward over the last few hours. Also, the other fields have changed remarkably in the last few hours. A strong positive vorticity maximum, located southwest of Wichita Falls at 2000 GMT (not shown) has approximately doubled in magnitude by 2200 GMT. The velocity convergence field has strengthened over the same 2-h period with an extensive axis of convergence (positive values) stretching along the Red River Valley at 2200 GMT. A similar pattern is noted in the moisture convergence field. Thus, many of the mesoscale ingredients for severe tornadic development are present just upstream from Wichita Falls 1–2 hours before the tornado occurs there.

b. Severe storm period 2: 0000–0200 GMT 11 April

The devastating Wichita Falls tornado started its 45 mile track at 2355 GMT 10 April southwest of the city and continued northeastward to Waurika, Oklahoma where it dissipated at 0100 GMT 11 April. Pressure and temperature analyses at 0000 and 0200 GMT are depicted in Fig. 7. The sub-synoptic low, which was located south of Childress at 2200 GMT, has moved eastward and is now west of Wichita Falls. This low has shown excellent temporal and spatial continuity. At 0200 GMT a new sub-synoptic low is located in the Abilene–San Angelo area. It developed between 0100 and 0200 GMT. In support of the second sub-synoptic low, time sections of pressure for Abilene and San Angelo are depicted in Fig. 8. The rapid pressure fall associated with the formation of this low occurs in San Angelo at 0120 GMT and in Abilene at 0130 GMT. Intense thunderstorm activity follows approximately two hours later. The 0000 and 0200 GMT temperature analyses continue to show the strong thermal ridge in west-central Texas. The strong temperature gradient, noted on the previous charts, has moved northward into southern Oklahoma by 0200 GMT.

Fig. 10 depicts the θ_E and vorticity fields for 0000

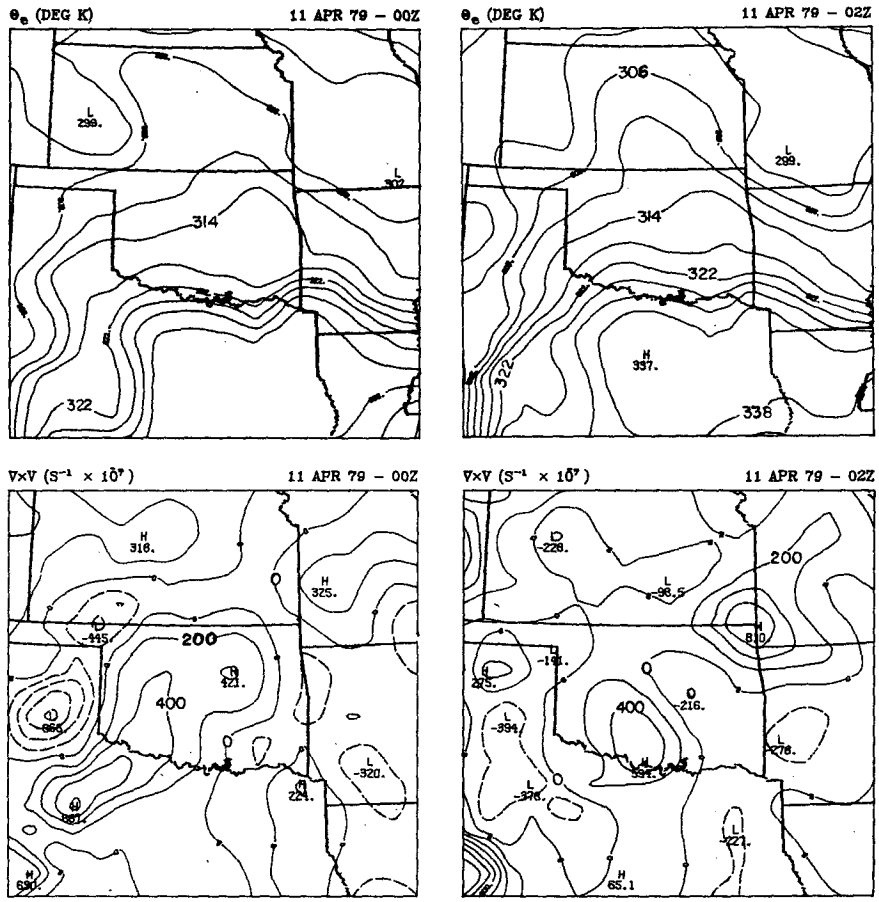

FIG. 10. Surface equivalent potential temperature θ_E and vorticity fields for 0000 GMT and 0200 GMT 11 April. Increments same as in Fig. 6.

and 0200 GMT. The θ_E analysis at 0000 GMT shows a trough in the isopleths in west-central Texas. This is a significant change from the 2200 GMT analysis (Fig. 6), when a θ_E maximum was observed in this area. This feature reflects the eastward branch of the dry tongue previously noted in the dewpoint depression. By 0200 GMT, the θ_E isopleths are once again packed tightly in western Texas. Note that the 322 K isopleth has retreated much farther west. The vorticity analysis for 0000 GMT shows a long band of positive vorticity centered along the axis of moist convective activity. Maxima exist in west-central Texas, northeast Oklahoma and southwest Missouri, suggesting the existence of mesoscale waves along this axis. It is interesting to note that Vincent and Homan (1983) identified three mesoscale pressure waves which propagated along the axis of moist convective activity and were correlated with heavy thunderstorms.

Fig. 11 depicts the velocity and dewpoint temperature convergence fields for the same times as in Fig. 10. In the velocity convergence field a strong, organized band of convergence exists over western Texas. This feature has a more organized structure and has strengthened from the previous set of charts. Another strong maximum is located along the Red River just east of Wichita Falls. The moisture convergence pattern is quite different from the velocity convergence, particularly in western Texas. At 0000 GMT the strongest band of moisture convergence extends in an east–west direction along the Red River Valley. Note that even though very strong velocity convergence is present in western Texas at 0000 GMT, the moisture convergence pattern in unfavorable for storm development. Recall that extremely dry air was penetrating into the Abilene area at this time. However, by 0200 GMT, approximately 30 minutes after the formation of the second sub-synoptic low, an axis of moisture convergence extends southwest from the Red River.

4. Summary and conclusions

Following the development of the two sub-synoptic lows, convection persisted in a long band stretching from central Texas northeastward to Missouri. The first low, which formed by 2000 GMT 10 April, was identifiable until at least 0300 GMT 11 April. Therefore, it had a lifetime of 7–8 hours. The second low, which developed between 0100 and 0200 GMT, was

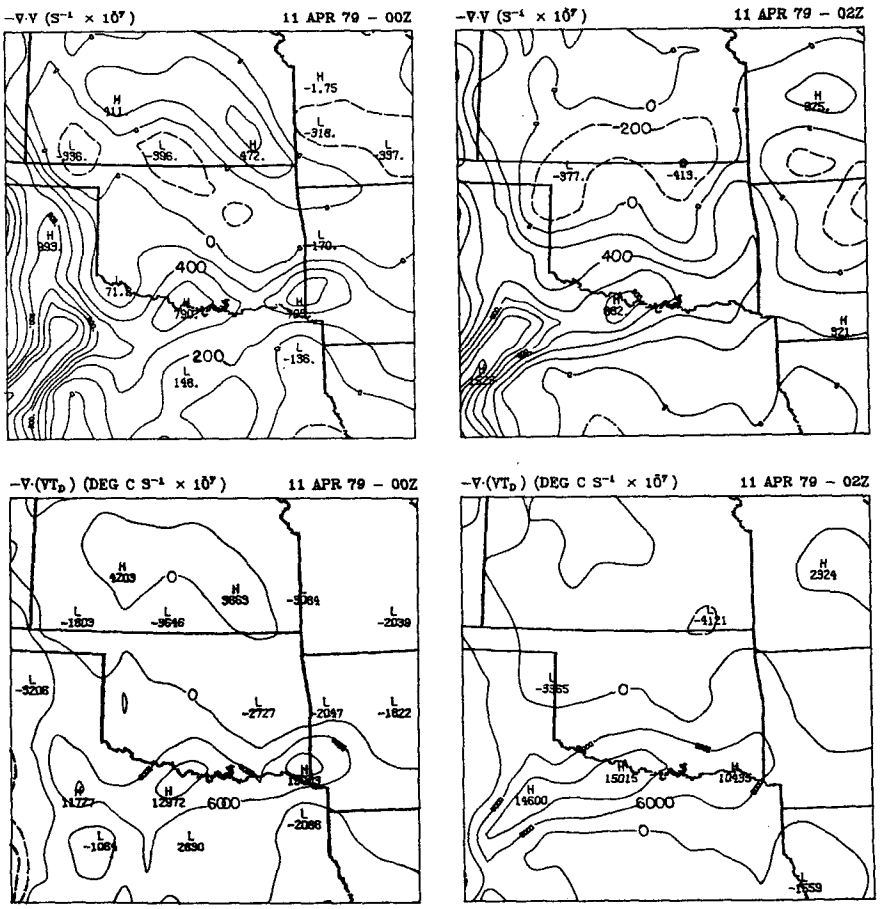

FIG. 11. Velocity and dewpoint temperature convergence at the surface for 0000 and 0200 GMT 11 April. Increments same as in Fig. 6.

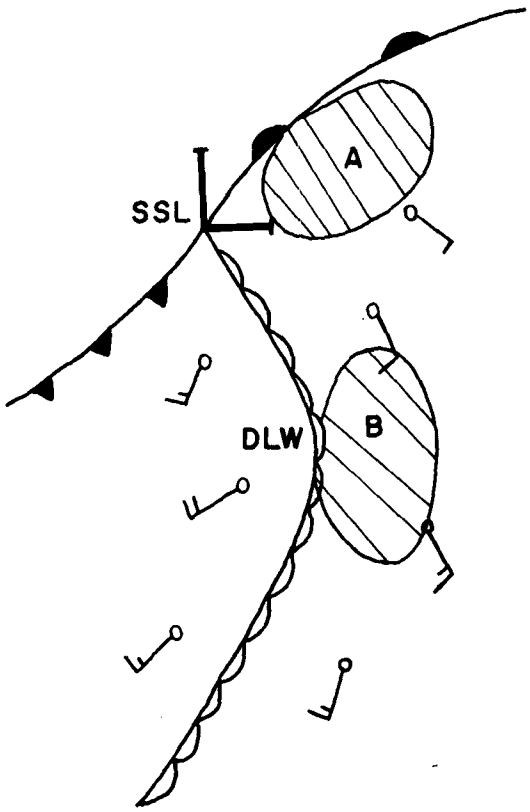

FIG. 12. Schematic of Tegtmeier's (1974) idealized Sub-Synoptic Low (SSL), Dry Line Wave (DLW) Model. Areas A and B (hatched) represent the first and second areas discussed in the text. Winds are in m s^{-1}.

not clearly identifiable in our 0400 GMT pressure analysis. Consequently, it appeared to have a much shorter lifetime than the first low.

Tegtmeier (1974) relates severe thunderstorm formation to an idealized sub-synoptic low (SSL)-dry line wave (DLW) model. According to Tegtmeier, there are two favorable areas for thunderstorm formation (Fig. 12). The first (area A) is located northeast of the SSL in a region where winds have backed to the southeast with respect to the ambient southerly flow east of the dry line. He characterizes these southeast winds as representing the sub-synoptic inflow vector. The importance of the inflow vector is to increase the moisture convergence northeast of the SSL which provides a favorable area for thunderstorm formation. The second area (B) is located on the moist side of an eastward dryline bulge. East of the bulge, winds back to a southeasterly direction enhancing the moisture convergence along the DLW. This model seems to fit particularly well with the present case study. The region of southeasterly winds was seen in Fig. 4. The Wichita Falls storm occurred in the first area (Area A) associated with the first sub-synoptic low, whereas the second swath of storms occurred east of the dryline bulge, between 0100 GMT and 0200 GMT, in conjunction with the second sub-synoptic low.

Acknowledgments. The authors express their sincere gratitude to Drs. Phillip J. Smith and John Snow for their helpful discussions and review of the manuscript and to Mr. Ray Brady, as well as Drs. Snow and David R. Smith, for their assistance in applying PROAM and its plotting routine. Special thanks are given to Grant Darkow of the University of Missouri for supplying the surface data. The authors also thank Mr. Richard Fulton for drafting the figures and Ms. Tanya Care for typing the manusript. The research was supported by the Meteorology Program, Division of Atmospheric Sciences, National Science Foundation under Grant ATM80-16169 issued to Purdue University.

REFERENCES

Alberty, R. L., D. W. Burgess and T. T. Fujita, 1980: Severe weather events of 10 April 1979. *Bull. Amer. Meteor. Soc.*, **61**, 1033–1034.

Barnes, S. L., 1964: A technique for maximizing detail in numerical weather map analysis. *J. Appl. Meteor.*, **3**, 396–409.

——, 1973: Mesoscale objective map analysis using weighted time-series observations. NOAA Tech. Memo. ERL NSSL-62, National Severe Storms Laboratory, Norman, OK 73069, 60 pp.

——, 1981: *SESAME 1979 Data User's Guide. Project Severe Environmental Storms and Mesoscale Experiment.* NOAA/ERL, Boulder, 236 pp.

Endlich, R. M., and R. L. Mancuso, 1968: Objective analysis of environmental conditions associated with severe thunderstorms and tornadoes. *Mon. Wea. Rev.*, **96**, 342–350.

Fujita, T., 1955: Results of detailed synoptic studies of squall lines. *Tellus*, **7**, 405–435.

——, H. Newstein and M. Tepper, 1956: Mesoanalysis: An important scale in the analysis of weather data. Research pap. No. 39, U.S. Department of Commerce, Government Printing Office, 83 pp.

Moore, J. T., and H. E. Fuelberg, 1981: A synoptic analysis of the first AVE–SESAME '79 period. *Bull. Amer. Meteor. Soc.*, **62**, 1577–1590.

Orlanski, I., 1975: A rational subdivision of scales for atmospheric processes. *Bull. Amer. Meteor. Soc.*, **56**, 527–530.

Smith, D. R., and F. W. Leslie, 1982: Evaluation of a Barnes-type objective analysis scheme for surface meteorological data. NASA Tech. Memo. No. TM-82509, Marshall Space Flight Center, Huntsville, 28 pp.

Tegtmeier, S. A., 1974: The role of the surface, sub-synoptic low pressure system in severe weather forecasting, M.S. thesis, School of Meteorology, University of Oklahoma, Norman, 66 pp.

Tepper, M., 1959: Mesometeorology—the link between macroscale atmospheric motions and local weather. *Bull. Amer. Meteor. Soc.*, **40**, 56–72.

Uccellini, L. W., and P. J. Kocin, 1981: Mesoscale aspects of jet streak coupling and implications for the short term forecasting of severe convective storms. *Proc. IAMAP Symp.*, Hamburg, ESA SP-165, European Space Agency, 375–379.

Vincent, D. G., and J. H. Homan, 1983: Mesoscale analysis of pressure and precipitation patterns during AVE–SESAME 1979, 10–11 April. *Bull. Amer. Meteor. Soc.*, **64**, 23–28.